ACS OMEGA

http://pubs.acs.org/journal/acsodf

Article

Rapid Quantitative Detection of Voriconazole in Human Plasma Using Surface-Enhanced Raman Scattering

Jing Liu, Wufeng Fan, Xiaoxia Lv,* and Cuijuan Wang*

Cite This: *ACS Omega* 2022, 7, 47634−47641

Read Online

ACCESS | Metrics & More | Article Recommendations

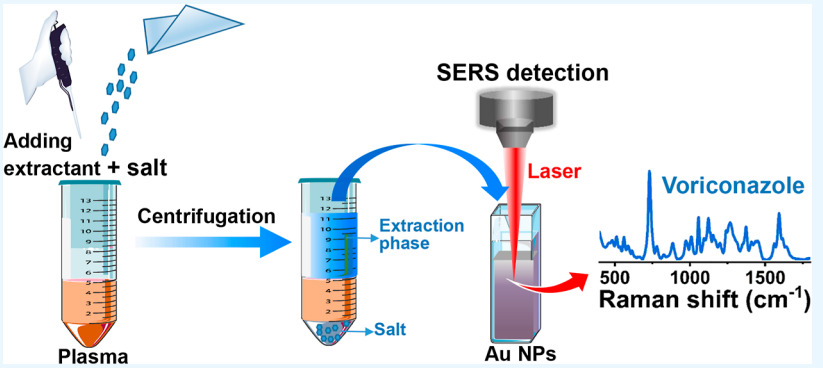

ABSTRACT: There is an increasing demand for rapid detection techniques for monitoring the therapeutic concentration of voriconazole (VRC) in human biological fluids. Herein, a rapid and selective surface-enhanced Raman scatting method for point-of-care determination of VRC in human plasma was developed *via* a portable Raman spectrometer. This approach has enabled the quantification of the VRC spiked into human plasma at clinical relevant concentrations. A gold nanoparticle solution (Au sol) was used as the SERS substrate, and the agglomerating conditions on its sensitivity were optimized. The method involves the formation of hot spots, and the signal of VRC molecules adsorbed on the surface of the SERS hot spot was amplified by 10^5. The calibration curve was linear in the range of 0.02−10 ppm, with satisfactory repeatability. The limit of detection was as low as 12.3 ppb. The variation in VRC spectra over time on different substrates demonstrated good reproducibility. Notably, the salting-out extraction method developed in this study was rapid and suitable for the quantitation of drugs in biological samples. Compared with traditional methods, this approach allows for the point-of-care quantification of VRC directly in a complex matrix, which may open up new exciting opportunities for future use of the SERS technique in clinical applications.

1. INTRODUCTION

Voriconazole (VRC) is a third-generation systemic triazole with broad-spectrum antifungal activity[1] and has been used as the first-line treatment for invasive fungal diseases.[2] It is designated chemically as (2*R*,3*S*)-2-(2,4-difluorophenyl)-3-(5-fluoro-4-pyrimidinyl)-1-(1*H*-1,2,4-triazol-1-yl)-2-butanol.[2] However, VRC exhibits extreme interindividual and intra-individual variations both in its efficacy and in its toxicity.[3] Plasma levels of VRC could vary by sex, age, genotype, and drug−drug interactions, showing a nonlinear pharmacokinetic profile with wide variability.[4] Previous clinical studies proved that VRC is rapidly absorbed following oral administration, with a maximum plasma concentration occurring 1−2 h after dosing and mainly excreted unchanged in urine and feces.[5] Under- and overdosing of VRC tend to influence the efficacy and safety of therapy. Plasma VRC concentrations higher than 5 or 6 ppm are associated with serious clinical events.[6] The most frequent adverse reactions induced by a high VRC level were visual disturbance, decreased vision, and liver toxicity.[7] Therefore, to optimize therapy efficiency while avoiding drug toxicity in individual patients, therapeutic monitoring of VRC is generally recommended.

At present, the detection of VRC in human biofluids such as serum, plasma, and urine is commonly achieved *via* the use of high-performance liquid chromatography (HPLC),[8] liquid chromatography−mass spectrometry (LC−MS),[9] and immunoassay.[8,10] Although the chromatography methods are reliable and accurate, the operations are complex and time-consuming, which affect the detection efficiency of therapeutic drug monitoring. In addition, professionally trained personnel with

Received: July 18, 2022
Accepted: December 6, 2022
Published: December 15, 2022

https://doi.org/10.1021/acsomega.2c04521
ACS Omega 2022, 7, 47634−47641

related background knowledge and expertise are required. Immunoassay cannot achieve the identification of the specific chemical structure of VRC.[8] These disadvantages hinder the development of new analytical protocols for on-site detection and monitoring of drugs in various biological fluids. To meet the urgent clinical needs, the development of a simple, rapid, assay for point-of-care detection of VRC is imperative.

Raman spectroscopy is a vibrational spectroscopy technique based on the interaction of light and chemical bonds.[11] It provides a highly specific molecular fingerprint for the identification and quantification of various analytes and is therefore considered to have great potential for application.[12] Surface-enhanced Raman spectroscopy (SERS) can realize rapid and trace level detection of analytes adsorbed on or near appropriately rough noble metal surfaces.[11] Previous studies have reported the potential and effectiveness of SERS for the analysis of drugs in human body fluids such as plasma,[13] serum,[14] urine,[15] and saliva,[16] which was considered an ideal technique for successfully measuring drugs. The application of a portable Raman spectrometer has greatly promoted the development of on-site SERS detection technology.[17] Therefore, combining SERS technology with portable instruments is an effective means to greatly facilitate the development of point-of-care detection methods.

Herein, we present a rapid SERS method for quantifying VRC in spiked human plasma samples using a portable Raman spectrometer. This approach involves using the well-known standard addition method, as well as an HPLC assay for additional benchmarking. Due to the complexity of the human plasma matrix, a simple salt-induced phase separation extraction method was developed to improve the selectivity and sensitivity. The results achieved by this approach clearly demonstrate the potential application of SERS for the detection of VRC as low as 12.3 ppb, which is sufficient for clinical applications. This assay has the advantage of being highly portable and can be developed as a point-of-care testing tool.

2. EXPERIMENTAL SECTION

2.1. Chemicals and Reagents. VRC (94.37%) was purchased from the National Institutes for Food and Drug Control (Beijing, China). Chloroauric acid ($HAuCl_4$) (99.5%), sodium citrate (99.0%), and other reagents were purchased from Sinopharm Chemical Reagent Co., Ltd. (Shanghai, China). These solutions and reagents were analytically pure and did not require further purification. Milli-Q water (18.2 MΩ cm) was used throughout the experiment.

2.2. Synthesis of Gold Nanoparticles. The gold nanoparticles (Au NPs) were synthesized according to a well-known citrate-reduction procedure according to a previous study[18] with slight changes. Briefly, 1 mL of 1% (w/v) $HAuCl_4$ was added to 99 mL of water and heated to boiling point under magnetic stirring at 600 rpm. Next, 1 mL of 1% (w/v) sodium citrate was added to the mixed solution, and the mixture was heated at boiling temperature for a further 20 min until a brick red nanogold colloid was obtained.

2.3. Instrumentation. SERS spectra were collected using a portable Raman spectrometer (QE Pro, Ocean Optics, USA), equipped with a 785 nm HeNe laser. All samples were analyzed within the spectral range of 400−2000 cm^{-1}, and the laser exposure time was set to 10 s for all samples. The excitation wavelength was 785 nm, and laser power was set as 200 mW. The uniformity and morphology of the synthesized NPs were examined by transmission electron microscopy (TEM) at an accelerating voltage of 100 kV (JEM-CXII). Optical absorption spectra were acquired using a Shimadzu 2600 ultraviolet−visible light (UV−vis) spectrometer at 25 °C.

2.4. Preparation of Solutions and Samples. Human plasma samples were obtained from The Second Affiliated Hospital of Shandong First Medical University and The Affiliated Hospital of Shandong University of Traditional Chinese medicine. From April to September 2022, blood samples were collected from 20 healthy volunteers (2 mL per person) and stored at 4 °C before use. The experiments were carried out in the laboratory of Shandong First Medical University. This study was approved by the Research Ethical Committee of The Second Affiliated Hospital of Shandong First Medical University (no. 2022-090) and conformed to the principles set out in the WMA Declaration of Helsinki.

A stock solution of VRC with a concentration of 2 mg/mL was prepared directly in ethanol. Serial dilution of VRC with plasma or water was then prepared using the stock solutions with final concentrations ranging from 20 ppb to 10 ppm. For quantification measurements, a pooled human plasma sample from volunteers was used and spiked with different VRC concentrations. For SERS detection, 50 μL of the VRC aqueous solution or extraction phase was first added to 940 μL of the Au sol and mixed thoroughly in a glass vial. Next, 10 μL of the aggregating agent was added and mixed thoroughly. Then, the reaction solution was transferred to a cuvette for SERS signal acquisition (Scheme 1).

Scheme 1. Scheme of the SERS-Based Quantitative VRC Analysis by Coupling Au NPs with a Portable Raman Spectrometer

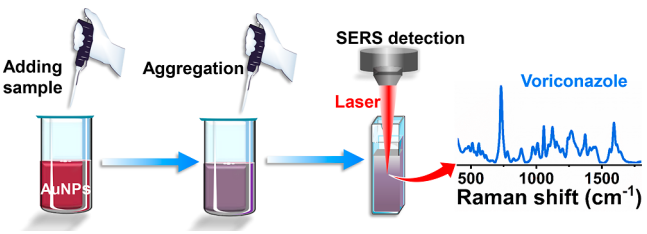

2.5. Extraction of VRC from Human Plasma. Acetonitrile (1.0 mL) was first mixed with 0.5 mL of the plasma sample and mixed for 10 s. Next, 0.2 g of sodium chloride was added in the mixture and vortexed for 30 s, followed by centrifugation at 5000 rpm for 3 min. After that, 50 μL of the separated acetonitrile phase was transferred to the Au sol for SERS measurements.

2.6. Estimation of the Enhancement Factor. The enhancement factor (EF) was estimated with 1 ppm of VRC using the equation $EF = (I_{SERS}/C_{SERS})/(I_{RS}/C_{RS})$, where I_{SERS} and I_{RS} indicate the SERS signal intensity of VRC at 730 cm^{-1} under SERS and non-SERS substrate conditions and C_{SERS} and C_{RS} are the corresponding concentrations, respectively.[19]

3. RESULTS AND DISCUSSION

3.1. Raman Characterization of VRC. Figure 1A displays the UV−vis spectra of colloidal Au NPs, Au NPs mixed with 1 ppm of VCR, and aggregated Au NPs after adding 1 ppm of VCR. TEM reveals spherical nanoparticles with a size of around 45−65 nm (Figure 1B). Figure 1C shows the chemical structure of VRC. The reference Raman spectrum of bulk solid

https://doi.org/10.1021/acsomega.2c04521
ACS Omega 2022, 7, 47634−47641

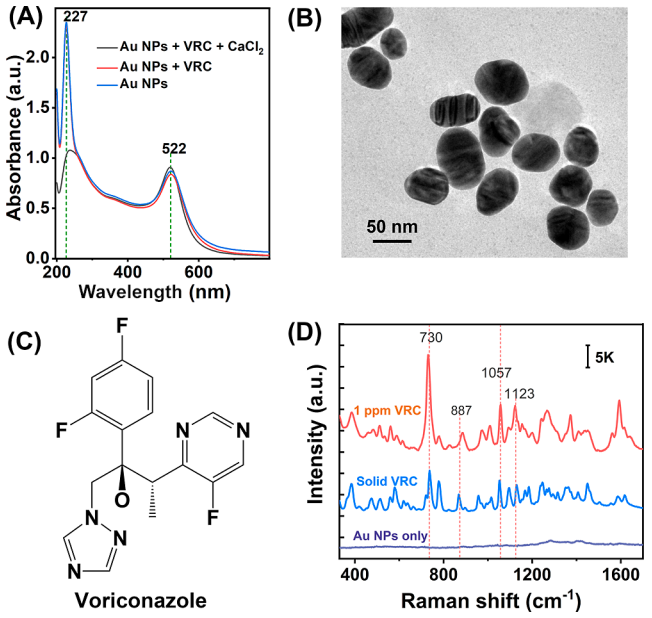

Figure 1. (A) UV−vis spectra of colloidal Au NPs, Au NPs mixed with 1 ppm of VCR, and aggregated Au NPs after addition of 1 ppm of VCR. (B) TEM images of Au NPs. (C) Chemical structure of VRC. (D) Raman spectrum of solid VRC and the SERS spectrum of 1 ppm aqueous VRC.

VRC and SERS aqueous spectrum of 1 ppm aqueous VRC enhanced by the Au sol were collected using a portable Raman spectrometer, respectively (Figure 1D). Characteristic Raman bands could be clearly observed mainly at 730, 887, 1057, and 1123 cm^{-1}. The bands at 730 and 887 cm^{-1} can be attributed to N−H bending vibrations,[20] and the band at approximately 1123 cm^{-1} corresponds to the C−N vibrations.[20] The SERS fingerprint peaks were largely consistent with those obtained from the solid VRC. Since the 730 cm^{-1} band was strongly enhanced and well separated, it was used as a quantitative signal in this study. Raman technology can obtain the fingerprint of the analyte, which ensures the specificity of the detection. Although other N−H-containing compounds also exhibit a shift of 730 cm^{-1}, their fingerprints differ due to the steric structures and other groups.

3.2. Optimization of SERS for Detection of VRC. It is well known that hot spots in metal nanogaps can generate strong SERS.[21] Therefore, the type and concentration of the aggregating agent are critical factors affecting the sensitivity of the SERS signal. The aim of this part was to determine the concentration at which nanoparticle aggregation occurred for salt while simultaneously gaining a better understanding of the cations and anions of the aggregating agent interacting with the nanoparticles to produce SERS enhancement. Four different aggregating agents were examined, including monovalent, divalent, and trivalent chloride, sulfate, and nitrate salts ($CaCl_2$, $Al_2(SO_4)_3$, KNO_3, and NaCl). First, 50 μL of the standard VRC solution was pipetted into 940 μL of the Au NP solution, followed by vortexing for 10 s. Next, 10 μL of salt solution with the same concentration (1.0 M) was added to the above solution and was mixed thoroughly for 10 s to induce aggregation. Then, the solution was transferred to a quartz cuvette for the SERS measurement. After the same concentration of salts was added, the color of the Au NPs changed from brick red to purplish gray, indicating the occurrence of aggregation.[21] Under the premise that other conditions remain unchanged, $CaCl_2$ generated the strongest SERS signal (Figure 2A).

In addition, $CaCl_2$ solutions with various concentrations (0.1−1.0 M) were used to optimize the aggregation reaction. As depicted in Figure 2B, the maximum signal was produced by $CaCl_2$ with a concentration of 1.0 M. Figure 2C shows the signal intensity of 730 cm^{-1} produced by various types of salt, while Figure 2D displays the signal strength of 730 cm^{-1} with various concentrations of $CaCl_2$. These results indicated that

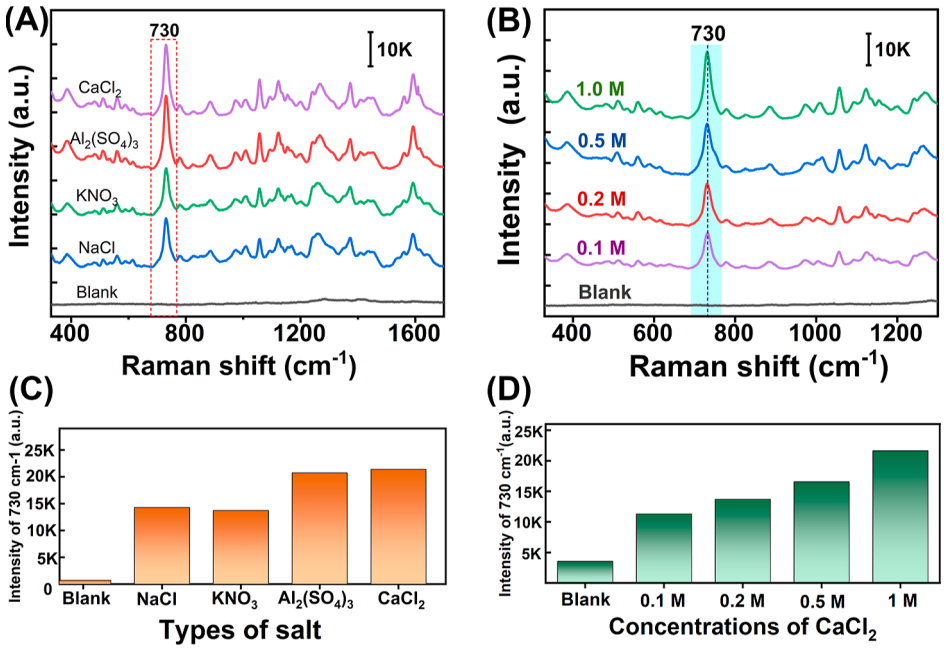

Figure 2. (A) SERS spectra of VRC were generated by four salts ($CaCl_2$, $Al_2(SO_4)_3$, KNO_3, and NaCl) with a concentration of 1.0 M. (B) Change in SERS intensity of VRC as a function of $CaCl_2$ concentration. Concentrations of $CaCl_2$ from bottom to top are ranging from 0.1 to 1.0 M. The signal intensity of 730 cm^{-1} produced by various types of salt (C) and $CaCl_2$ with different concentrations (D).

https://doi.org/10.1021/acsomega.2c04521
ACS Omega 2022, 7, 47634−47641

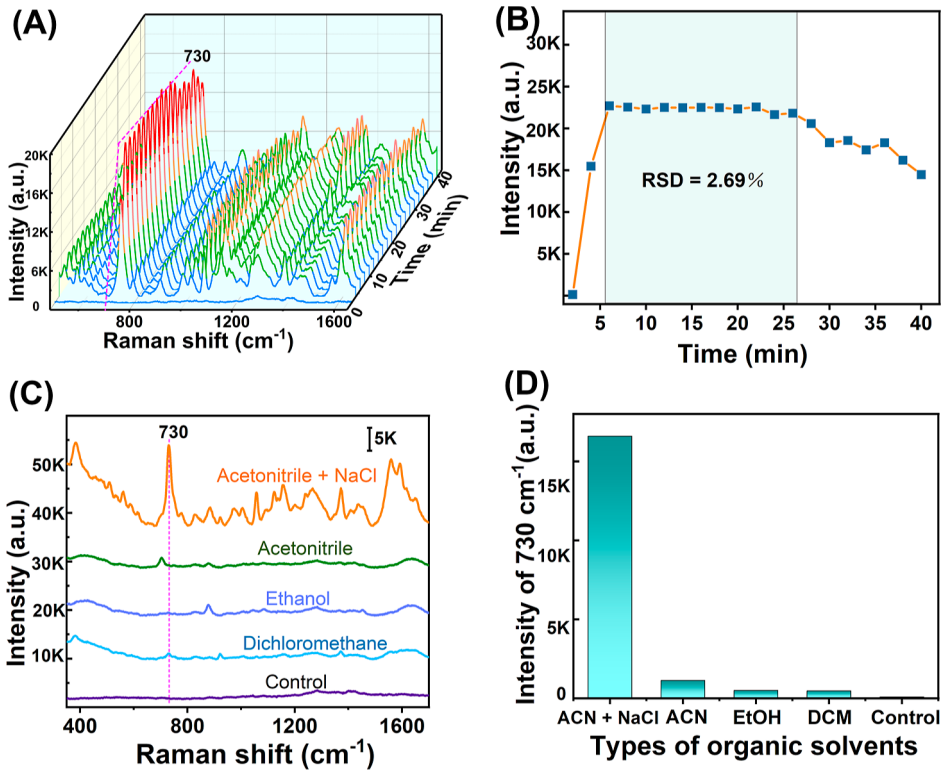

Figure 3. (A) Temporal evolution of the SERS spectra of VRC recorded after addition of 1 M $CaCl_2$ into VRC and the Au NP mixture. (B) Effect of the reaction time on the SERS intensity of the 730 cm^{-1} peak. (C) SERS characterization of the impact of types of organic solvents on the extraction of VRC from human plasma. (D) Effect of various types of solvents on the intensity of the 730 cm^{-1} peak. Plasma sample without extraction was used as a control.

the strongest signal was produced by $CaCl_2$ with a concentration of 1.0 M and was therefore chosen as the aggregating agent in the following experiment.

The addition of salt to the Au NP solution would induce the aggregation due to the strong electrostatic interaction of positively charged VRC and the negatively charged Au NPs.[21] In this way, electromagnetic (EM) "hot spots" could be fabricated, and a large EM coupling effect was produced at the hot spots between Au NPs,[21,22] resulting in an enhancement of SERS intensity of VRC. Studies have shown that divalent and trivalent cations induce the stronger aggregation of gold nanoparticles than monovalent cations.[21] This is because the addition of aggregating salts decreases the zeta potential of the NPs and reduces the electrostatic repulsion between the particles. The stability of the colloidal solution is destabilized, and the aggregate-forming particles collide, resulting in the formation of hot spots where strong surface-enhanced resonances occur.

Reaction time is also an important experimental parameter that needs to be optimized. In this study, the SERS signal was continuously collected for 40 min, and the effect of aggregation time on the SERS intensity is displayed in Figure 3A,B. The signal increased for the first 6 min, remained steady for the next 20 min, and then decreased slowly thereafter. As the signal was stable from 6 to 26 min, the aggregation was allowed to occur for 20 min. Moreover, as the signal is steady for a sufficiently long period (20 min), the proposed method not only allows for fast VRC detection but also ensures reliable and reproducible measurements. The EF of Au NPs was determined to be 3.99×10^5.

3.3. Extraction of VRC from Real Blood Plasma. The above optimization of the coagulation reaction was to increase the number of hot spots and further improve the chances of capturing target molecules.[23] However, the analyte may not be able to access the hot spot due to occupancy by impurities or ligands.[24] The detection of drugs in human blood is complicated by the presence of interfering substances such as organic salts and proteins, which may generate large amounts of background noise and prevent VRC from reaching the enhanced hot spots of the SERS substrate.[25] In general, signal interference from blood components can lead to poor sensitivity, and the strong interaction of blood components with precious metal surfaces can block plasma spots.[26] Therefore, reducing the nonspecific interactions and adsorption of proteins, enzymes, hormones, and other blood components to metal surfaces can increase SERS substrate sensitivity.[13] During the pretreatment of complex matrix samples, it is important to select an appropriate extraction solvent to separate and preconcentrate target analytes from samples.

Here, a pretreatment step for VRC extraction from real human plasma was performed to optimize the detection sensitivity. The extraction solvent was selected based on certain requirements, such as miscibility with the sample and extraction capability of the target analyte. The extraction performance of four extractants [ethanol, acetonitrile, dichloromethane, and acetonitrile plus sodium chloride (NaCl)] was evaluated, while other experimental variables mentioned in the previous section were kept constant. According to Figure 3C,D, only acetonitrile plus NaCl showed good phase

https://doi.org/10.1021/acsomega.2c04521
ACS Omega 2022, 7, 47634−47641

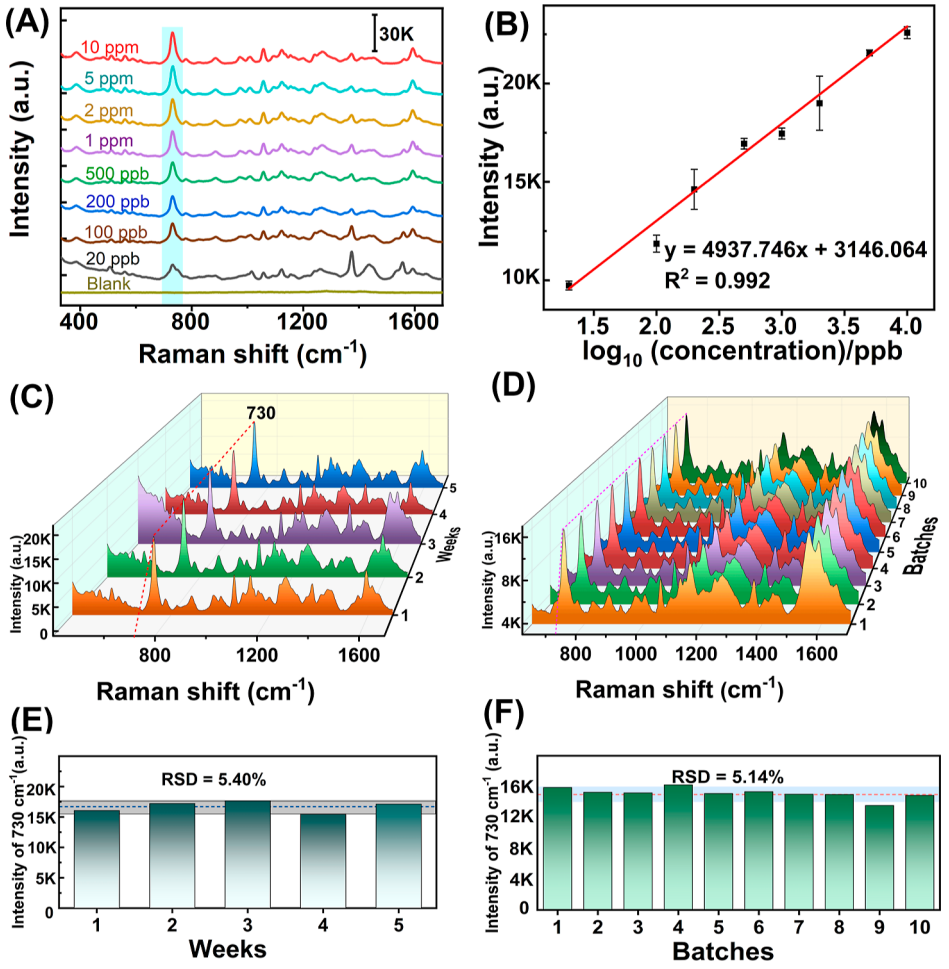

Figure 4. (A) SERS spectra of the VRC aqueous solution with different concentrations. (B) SERS intensity at 730 cm^{-1} vs the logarithmic concentrations of VRC. Error bars equal to the standard deviations obtained from three measurements. (C) Reproducibility measurements of SERS signal for detection of VRC (1 ppm) from the same batches within 5 weeks. (D) SERS signals produced by 10 different batches of the substrate. (E,F) show the intensity of peak at 730 cm^{-1} corresponding to (C,D).

separation and comparable extraction capacity of VRC and thus was selected as the extraction solvent in this study.

It is known that water and acetonitrile are miscible under normal temperature and pressure conditions.[27] However, after the addition of salt, the mixture of water and acetonitrile tends to undergo liquid−liquid phase separation into a water-rich phase and an acetonitrile-rich phase.[28] This phenomenon, known as salting-out-assisted liquid−liquid extraction (SALLE), has great potential in sample preparation.[27,29] The addition of salt increases the partitioning of the analyte in the organic phase by reducing the solubility of hydrophilic compounds in the aqueous phase through the salting-out effect.[29] Both high concentrations of salts and organic solvents in the SALLE system can effectively precipitate proteins prior to phase separation, and most salts, matrix components, and particulate residues remain in the aqueous phase during phase separation.[30] This technology has been initially studied in the detection of food[27] and personal care products.[29] Compared to traditional liquid−liquid extraction and solid-phase extraction, SALLE has the advantage of being more efficient and environmentally friendly, showing great potential for applications in biological fluid sample preparation.

3.4. Rapid Quantitative Analysis of VRC in Human Plasma. To demonstrate the feasibility of quantitatively detecting VRC levels using SERS, aqueous solutions with different VRC concentration gradients were added to the Au sol, and the SERS response was recorded. At and above 20 ppb, the characteristic Raman bands of VRC could be clearly identified (Figure 4A). The VRC band at 730 cm^{-1} as a function of concentration is shown in Figure 4B, displaying a clear linear intensity dependence with a correlation coefficient of 0.992 ($p < 0.05$). The limit of detection (LOD) of this method was calculated to be 12.3 ppb, which is sufficient for therapeutic drug monitoring.

To verify the feasibility of the developed method, the recovery of VRC in real plasma was investigated. Spiked plasma samples of known VRC concentrations (100, 500, and 1000 ppb) were added to the plasma to mimic the VRC content in clinical samples. As mentioned in Table 1, the average recovery rates of VRC in plasma samples for

Table 1. Recoveries in Spiked Human Plasma with Different Concentrations

spiked levels (ppb) (ppb)	found (ppb)	recovery (%)	RSD (%)[a]
1000	811.2 ± 128.2	81.12	15.81
500	502.2 ± 44.30	100.4	8.827
100	94.83 ± 3.617	94.83	3.818

[a]SD, standard deviation; RSD, relative standard deviation.

https://doi.org/10.1021/acsomega.2c04521
ACS Omega 2022, 7, 47634−47641

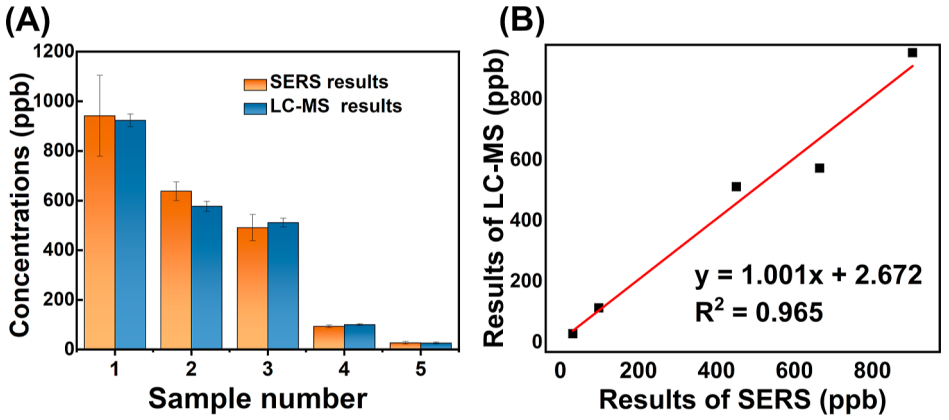

Figure 5. (A) Comparison of the results of two methods for detecting five concentrations of VRC in human plasma. (B) Linear correlation between the quantitative data of this proposed SERS approach and an HPLC method.

concentrations of 100, 500, and 1000 ppb were 81.12, 100.44, and 94.83% (with RSDs of 15.81, 8.82, and 3.81%), respectively. The recovery rates were sufficient for the clinical applications. Although the RSD was a bit large, the advantages of easy extraction and fast detection make up for it. Minimal human manual operation, few working steps, and short extraction time suppressed most of existing methods.

3.5. Reproducibility of Sensing. For effective quantitative measurements, the SERS signal needs to be stable and reproducible. The reproducibility of SERS signals is extremely important for the SERS biosensing strategy. However, the presence of large biomolecules is likely to affect the sensitivity and reproducibility of SERS sensing due to possible blocking of the Au surface.[31] In this study, SERS reproducibility was first studied by measuring the variation in the SERS signals produced by the same batch of the Au sol within 5 weeks. The results showed the good stability of the signal obtained with the same batch of the Au sol over a period of 35 days (Figure 4C,E), with a RSD of 5.40%. Next, samples spiked with the same concentrations of VRC (1 ppm) were tested using 10 different batches of the Au sol (Figure 4D,F), with a RSD of 5.14%. These results indicate sufficient stability and reproducibility of this proposed method for applications and thus has great potential for monitoring the therapeutic blood level of VRC.

3.6. Comparison of the Present Method with Other Methods. For cross-validation of the SERS strategy, the prepared samples were analyzed by an HPLC approach according to a previous study.[10] Spiked plasma VRC samples (concentrations of 0.03, 0.1, 0.5, 0.6, and 1.0 ppm) were detected based on a double-blind fashion. Figure 5 shows an HPLC versus SERS plot for five analyses, reflecting a satisfactory linear trend with an R^2 of 0.965. Moreover, SERS provides the advantages of efficiency and convenience, which has great potential of realizing on-site and point-of-care detection of VRC.

Most of the existing technologies for detecting VRC in biofluids are generally performed only in the laboratory (Table 2). These techniques usually require sophisticated instrumentation and time-consuming pretreatments, which largely hinder the achievement of rapid on-site determination. In order to meet the requirements of clinical applications, related analytical methods urgently need improvement in order to become simple, rapid, and user-friendly. This method could achieve VRC signal acquisition within 6 min with a simple preprocessing procedure and has the advantages of less time requirement, rapid acquisition of specific fingerprints, and the merit of portability. Therefore, this method could be used as a good alternative to existing methods for the detection of VRC in biological samples, meeting the urgent clinical need for point-of-care detection.

Table 2. Comparison of Different Methods for Detecting VRC in Biological Samples

method	media	pre-processing operation (time)	detection limit (ppb)	references
SERS	plasma	salt-induced liquid−liquid separation	12.5	this study
UPLC-MS/MS	serum	solvent extraction	65	32
HPLC	plasma	solvent extraction	44	33
HPLC	plasma	solid-phase extraction	50	34
paper spray MS/MS	plasma	paper spray cartridge	20	35
LC/MS/MS	blood	solid-phase extraction	50	36

4. CONCLUSIONS

There is a real urgent unmet need for rapid detection of VRC in patients. This study developed a rapid and simple approach for extraction and quantification of VRC in human plasma. The application of the salt-induced extraction approach reduced the redistribution of the extractant into the aqueous phase during collection, reduces the organic phase collection time, and increases the extraction efficiency. As compared to other methodologies, the method developed and optimized in this study has several advantages, such as high extraction efficiency, easily performed with an inexpensive portable Raman spectrometer, point-of-care accessibility, and a short detection time. It was successfully applied to determine VRC with satisfactory recovery (81.12−100.44%) and low LOD (12.3 ppb) in spiked human plasma, which are sufficient for clinical needs. It is highly notable that the proposed method realized sensitive identification and quantification of VRC with excellent reproducibility, satisfactory recovery, and stability. We believe that this new SERS analytical approach could easily be translated into an on-site, rapid detection tool for monitoring the therapeutic VRC level.

https://doi.org/10.1021/acsomega.2c04521
ACS Omega 2022, 7, 47634−47641

AUTHOR INFORMATION

Corresponding Authors

Xiaoxia Lv − *Central Sterile Supply Department, Affiliated Hospital of Shandong University of Traditional Chinese Medicine, Jinan, Shandong 250014, P. R. China;* orcid.org/0000-0002-1775-4592; Email: xx617013@163.com

Cuijuan Wang − *Physical and Chemical Laboratory, Shandong Academy of Occupational Health and Occupational Medicine, Shandong First Medical University & Shandong Academy of Medical Sciences, Jinan 250000, P. R. China*; Email: wangcuijuan@sdfmu.edu.cn

Authors

Jing Liu − *Department of Clinical Laboratory, The Second Affiliated Hospital of Shandong First Medical University, Shandong First Medical University and Shandong Academy of Medical Sciences, Taian, Shandong 271000, P. R. China*

Wufeng Fan − *Outpatient Department, Affiliated Hospital of Shandong University of Traditional Chinese Medicine, Jinan, Shandong 250014, P. R. China*

Complete contact information is available at: https://pubs.acs.org/10.1021/acsomega.2c04521

Author Contributions

J.L.: writing—original draft, performing the experiments, and data curation. W.F.: software, validation. X.L.: conceptualization, supervision. C.W.: methodology, data curation, writing—review & editing. All authors have given approval to the final version of the manuscript.

Notes

The authors declare no competing financial interest.

ACKNOWLEDGMENTS

This work was financially supported by the Natural Science Foundation of Shandong Province (grant no. ZR2017MH097); Medical and Health Science and Technology Development Plan of Shandong Province [grant no. 202112070425]; and Traditional Chinese Medicine Project of Shandong Province [grant no. 2021M152].

REFERENCES

(1) Pallet, N.; Loriot, M. A. Voriconazole pharmacogenetics. *Lancet* **2021**, *398*, 578.

(2) Maertens, J. A.; Raad, I. I.; Marr, K. A.; Patterson, T. F.; Kontoyiannis, D. P.; Cornely, O. A.; Bow, E. J.; Rahav, G.; Neofytos, D.; Aoun, M.; Baddley, J. W.; Giladi, M.; Heinz, W. J.; Herbrecht, R.; Hope, W.; Karthaus, M.; Lee, D. G.; Lortholary, O.; Morrison, V. A.; Oren, I.; Selleslag, D.; Shoham, S.; Thompson, G. R., 3rd; Lee, M.; Maher, R. M.; Schmitt-Hoffmann, A. H.; Zeiher, B.; Ullmann, A. J. Isavuconazole versus voriconazole for primary treatment of invasive mould disease caused by Aspergillus and other filamentous fungi (SECURE): a phase 3, randomised-controlled, non-inferiority trial. *Lancet* **2016**, *387*, 760−769.

(3) (a) Racette, A. J.; Roenigk, H. H., Jr.; Hansen, R.; Mendelson, D.; Park, A. Photoaging and phototoxicity from long-term voriconazole treatment in a 15-year-old girl. *J. Am. Acad. Dermatol.* **2005**, *52*, S81−S85. (b) Hedrick, J.; Droz, N. Voriconazole-Induced Periostitis. *N. Engl. J. Med.* **2019**, *381*, No. e30.

(4) Neely, M.; Rushing, T.; Kovacs, A.; Jelliffe, R.; Hoffman, J. Voriconazole pharmacokinetics and pharmacodynamics in children. *Clin. Infect. Dis.* **2010**, *50*, 27−36.

(5) Bellmann, R. Pharmacodynamics and pharmacokinetics of antifungals for treatment of invasive aspergillosis. *Curr. Pharm. Des.* **2013**, *19*, 3629−3647.

(6) Gómez-López, A.; Cendejas-Bueno, E.; Cuesta, I.; Rodríguez, J.; Rodríguez-Tudela, J. L.; Gutiérrez-Altés, A.; Cuenca-Estrella, M. Voriconazole serum levels measured by high-performance liquid chromatography: a monocentric study in treated patients. *Med. Mycol.* **2012**, *50*, 439−445.

(7) Tang, D.; Yan, M.; Song, B. L.; Zhao, Y. C.; Xiao, Y. W.; Wang, F.; Liang, W.; Zhang, B. K.; Chen, X. J.; Zou, J. J.; Tian, Y.; Wang, W. L.; Jiang, Y. F.; Gong, G. Z.; Zhang, M.; Xiang, D. X. Population pharmacokinetics, safety and dosing optimization of voriconazole in patients with liver dysfunction: A prospective observational study. *Br. J. Clin. Pharmacol.* **2021**, *87*, 1890−1902.

(8) Peña-Lorenzo, D.; Rebollo, N.; Sánchez-Hernández, J. G.; Zarzuelo-Castañeda, A. Comparison of ultra-performance liquid chromatography and ARK immunoassay for therapeutic drug monitoring of voriconazole. *Ann. Clin. Biochem.* **2021**, *58*, 657−660.

(9) (a) Lu, Q.; He, X.; Fang, J.; Shi, K.; Hu, F.; Bian, X.; Wang, X. Simultaneous determination of linezolid and voriconazole serum concentrations using liquid chromatography-tandem mass spectrometry. *J. Pharmaceut. Biomed. Anal.* **2022**, *212*, 114659. (b) Xie, S.; Ye, L.; Ye, X.; Lin, G.; Xu, R. A. Inhibitory effects of voriconazole, itraconazole and fluconazole on the pharmacokinetic profiles of ivosidenib in rats by UHPLC-MS/MS. *J. Pharm. Biomed. Anal.* **2020**, *187*, 113353.

(10) Cattoir, L.; Fauvarque, G.; Degandt, S.; Ghys, T.; Verstraete, A. G.; Stove, V. Therapeutic drug monitoring of voriconazole: validation of a novel ARK immunoassay and comparison with ultra-high performance liquid chromatography. *Clin. Chem. Lab. Med.* **2015**, *53*, e135−e139.

(11) Zong, C.; Xu, M.; Xu, L. J.; Wei, T.; Ma, X.; Zheng, X. S.; Hu, R.; Ren, B. Surface-Enhanced Raman Spectroscopy for Bioanalysis: Reliability and Challenges. *Chem. Rev.* **2018**, *118*, 4946−4980.

(12) Xu, K.; Zhou, R.; Takei, K.; Hong, M. Toward Flexible Surface-Enhanced Raman Scattering (SERS) Sensors for Point-of-Care Diagnostics. *Adv. Sci.* **2019**, *6*, 1900925.

(13) Bonifacio, A.; Dalla Marta, S.; Spizzo, R.; Cervo, S.; Steffan, A.; Colombatti, A.; Sergo, V. Surface-enhanced Raman spectroscopy of blood plasma and serum using Ag and Au nanoparticles: a systematic study. *Anal. Bioanal. Chem.* **2014**, *406*, 2355−2365.

(14) Göksel, Y.; Zor, K.; Rindzevicius, T.; Thorhauge Als-Nielsen, B. E.; Schmiegelow, K.; Boisen, A. Quantification of Methotrexate in Human Serum Using Surface-Enhanced Raman Scattering-Toward Therapeutic Drug Monitoring. *ACS Sens.* **2021**, *6*, 2664−2673.

(15) Wang, H.; Xue, Z.; Wu, Y.; Gilmore, J.; Wang, L.; Fabris, L. Rapid SERS Quantification of Trace Fentanyl Laced in Recreational Drugs with a Portable Raman Module. *Anal. Chem.* **2021**, *93*, 9373−9382.

(16) Yang, T.; Guo, X.; Wang, H.; Fu, S.; wen, Y.; Yang, H. Magnetically optimized SERS assay for rapid detection of trace drug-related biomarkers in saliva and fingerprints. *Biosens. Bioelectron.* **2015**, *68*, 350−357.

(17) (a) Lin, S.; Hasi, W.; Lin, X.; Han, S.; Xiang, T.; Liang, S.; Wang, L. Lab-On-Capillary Platform for On-Site Quantitative SERS Analysis of Surface Contaminants Based on Au@4-MBA@Ag Core-Shell Nanorods. *ACS Sens.* **2020**, *5*, 1465−1473. (b) Zhu, W.; Wen, B. Y.; Jie, L. J.; Tian, X. D.; Yang, Z. L.; Radjenovic, P. M.; Luo, S. Y.; Tian, Z. Q.; Li, J. F. Rapid and low-cost quantitative detection of creatinine in human urine with a portable Raman spectrometer. *Biosens. Bioelectron.* **2020**, *154*, 112067.

(18) Cao, X.; Hong, S.; Jiang, Z.; She, Y.; Wang, S.; Zhang, C.; Li, H.; Jin, F.; Jin, M.; Wang, J. SERS-active metal-organic frameworks with embedded gold nanoparticles. *Analyst* **2017**, *142*, 2640−2647.

(19) Lu, L.; Zhang, J.; Jiao, L.; Guan, Y. Large-Scale Fabrication of Nanostructure on Bio-Metallic Substrate for Surface Enhanced Raman and Fluorescence Scattering. *Nanomaterials* **2019**, *9*, 916.

(20) Westley, C.; Xu, Y.; Thilaganathan, B.; Carnell, A. J.; Turner, N. J.; Goodacre, R. Absolute Quantification of Uric Acid in Human

Urine Using Surface Enhanced Raman Scattering with the Standard Addition Method. *Anal. Chem.* **2017**, *89*, 2472−2477.
(21) Mostowtt, T.; Munoz, J.; McCord, B. An evaluation of monovalent, divalent, and trivalent cations as aggregating agents for surface enhanced Raman spectroscopy (SERS) analysis of synthetic cannabinoids. *Analyst* **2019**, *144*, 6404−6414.
(22) Li, M.; Cushing, S. K.; Zhou, G.; Wu, N. Molecular hot spots in surface-enhanced Raman scattering. *Nanoscale* **2020**, *12*, 22036−22041.
(23) Lu, H.; Zhu, L.; Zhang, C.; Chen, K.; Cui, Y. Mixing Assisted "Hot Spots" Occupying SERS Strategy for Highly Sensitive In Situ Study. *Anal. Chem.* **2018**, *90*, 4535−4543.
(24) Shin, Y.; Song, J.; Kim, D.; Kang, T. Facile Preparation of Ultrasmall Void Metallic Nanogap from Self-Assembled Gold-Silica Core-Shell Nanoparticles Monolayer via Kinetic Control. *Adv. Mater.* **2015**, *27*, 4344−4350.
(25) Panikar, S. S.; Ramírez-García, G.; Sidhik, S.; Lopez-Luke, T.; Rodriguez-Gonzalez, C.; Ciapara, I. H.; Castillo, P. S.; Camacho-Villegas, T.; De la Rosa, E. Ultrasensitive SERS Substrate for Label-Free Therapeutic-Drug Monitoring of Paclitaxel and Cyclophosphamide in Blood Serum. *Anal. Chem.* **2019**, *91*, 2100−2111.
(26) Xu, L. J.; Zong, C.; Zheng, X. S.; Hu, P.; Feng, J. M.; Ren, B. Label-free detection of native proteins by surface-enhanced Raman spectroscopy using iodide-modified nanoparticles. *Anal. Chem.* **2014**, *86*, 2238−2245.
(27) da Silva, W. P.; de Oliveira, L. H.; Santos, A. L. D.; Ferreira, V. S.; Trindade, M. A. G. Sample preparation combined with electroanalysis to improve simultaneous determination of antibiotics in animal derived food samples. *Food Chem.* **2018**, *250*, 7−13.
(28) Li, M.; Zhuang, B.; Lu, Y.; An, L.; Wang, Z. G. Salt-Induced Liquid-Liquid Phase Separation: Combined Experimental and Theoretical Investigation of Water-Acetonitrile-Salt Mixtures. *J. Am. Chem. Soc.* **2021**, *143*, 773−784.
(29) Chen, M. J.; Liu, Y. T.; Lin, C. W.; Ponnusamy, V. K.; Jen, J. F. Rapid determination of triclosan in personal care products using new in-tube based ultrasound-assisted salt-induced liquid-liquid microextraction coupled with high performance liquid chromatography-ultraviolet detection. *Anal. Chim. Acta* **2013**, *767*, 81−87.
(30) Tang, Y. Q.; Weng, N. Salting-out assisted liquid-liquid extraction for bioanalysis. *Bioanalysis* **2013**, *5*, 1583−1598.
(31) Guselnikova, O.; Lim, H.; Na, J.; Eguchi, M.; Kim, H. J.; Elashnikov, R.; Postnikov, P.; Svorcik, V.; Semyonov, O.; Miliutina, E.; Lyutakov, O.; Yamauchi, Y. Enantioselective SERS sensing of pseudoephedrine in blood plasma biomatrix by hierarchical mesoporous Au films coated with a homochiral MOF. *Biosens. Bioelectron.* **2021**, *180*, 113109.
(32) Basu, S. S.; Petrides, A.; Mason, D. S.; Jarolim, P. A rapid UPLC-MS/MS assay for the simultaneous measurement of fluconazole, voriconazole, posaconazole, itraconazole, and hydroxyitraconazole concentrations in serum. *Clin. Chem. Lab. Med.* **2017**, *55*, 836−844.
(33) Michael, C.; Teichert, J.; Preiss, R. Determination of voriconazole in human plasma and saliva using high-performance liquid chromatography with fluorescence detection. *J. Chromatogr., B* **2008**, *865*, 74−80.
(34) Bashir, K.; Chen, G.; Han, J.; Shu, H.; Cui, X.; Wang, L.; Li, W.; Fu, Q. Preparation of magnetic metal organic framework and development of solid phase extraction method for simultaneous determination of fluconazole and voriconazole in rat plasma samples by HPLC. *J. Chromatogr., B* **2020**, *1152*, 122201.
(35) Skaggs, C. L.; Ren, G. J.; Elgierari, E. T. M.; Sturmer, L. R.; Shi, R. Z.; Manicke, N. E.; Kirkpatrick, L. M. Simultaneous quantitation of five triazole anti-fungal agents by paper spray-mass spectrometry. *Clin. Chem. Lab. Med.* **2020**, *58*, 836−846.
(36) Martial, L. C.; van den Hombergh, E.; Tump, C.; Halmingh, O.; Burger, D. M.; van Maarseveen, E. M.; Brüggemann, R. J.; Aarnoutse, R. E. Manual punch versus automated flow-through sample desorption for dried blood spot LC-MS/MS analysis of voriconazole. *J. Chromatogr., B* **2018**, *1089*, 16−23.

https://doi.org/10.1021/acsomega.2c04521
ACS Omega 2022, 7, 47634−47641